

Advanced magnetic tunnel junctions based on CoFeB/MgO interfacial perpendicular anisotropy

S. Ikeda^{1,2}

M. Yamanouchi¹, H. Sato¹, K. Miura^{3,1,2}, K. Mizunuma², H. Yamamoto³, R. Koizumi²,
H. D. Gan¹, S. Kanai², J. Hayakawa³, F. Matsukura^{1,2}, H. Ohno^{1,2}

¹ Center for Spintronics Integrated Systems (CSIS), Tohoku Univ.

² Laboratory for Nanoelectronics and Spintronics, RIEC, Tohoku Univ.

³ Central Research Laboratory, Hitachi, Ltd.

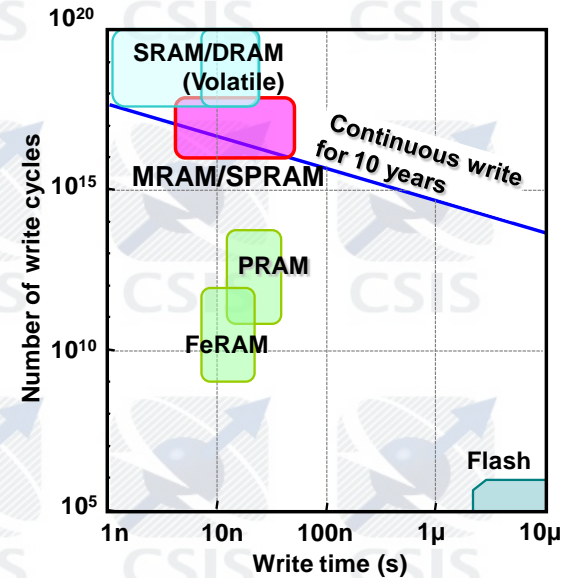
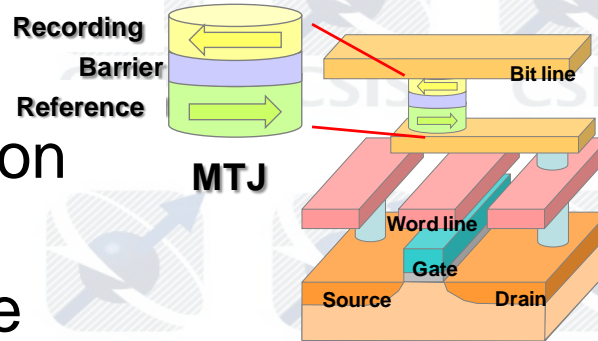
Acknowledgement: This work was supported by the project "Research and Development of Ultra-low Power Spintronics-based VLSIs" under the FIRST Program of JSPS.

Spintronics devices

(Expectation as low power consumption devices)

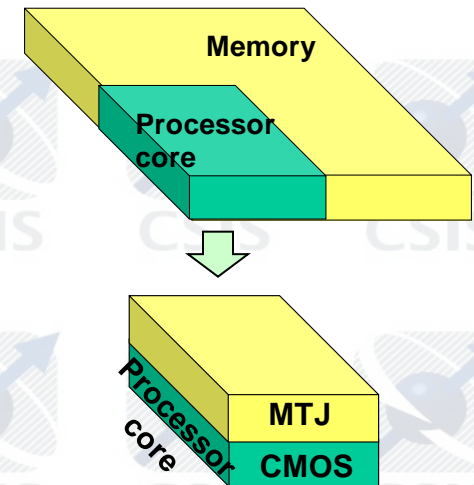
- Magnetoresistive RAMs (MRAMs)
SPin transfer torque RAMs (SPRAMs)

- ✓ Nonvolatility
- ✓ High speed operation
- ✓ Virtually unlimited write endurance



- Logic-in-memory architecture

- ✓ Reduction of leak current (static power)
- ✓ Reduction of interconnection delay



Mochizuki *et al.*, IEICE Transactions on Fundamentals, E88-A (2005) 1408.

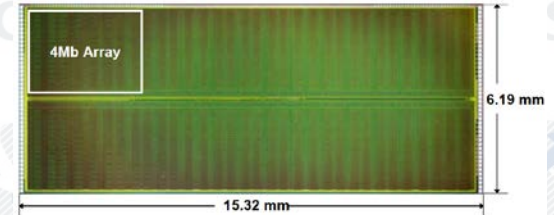
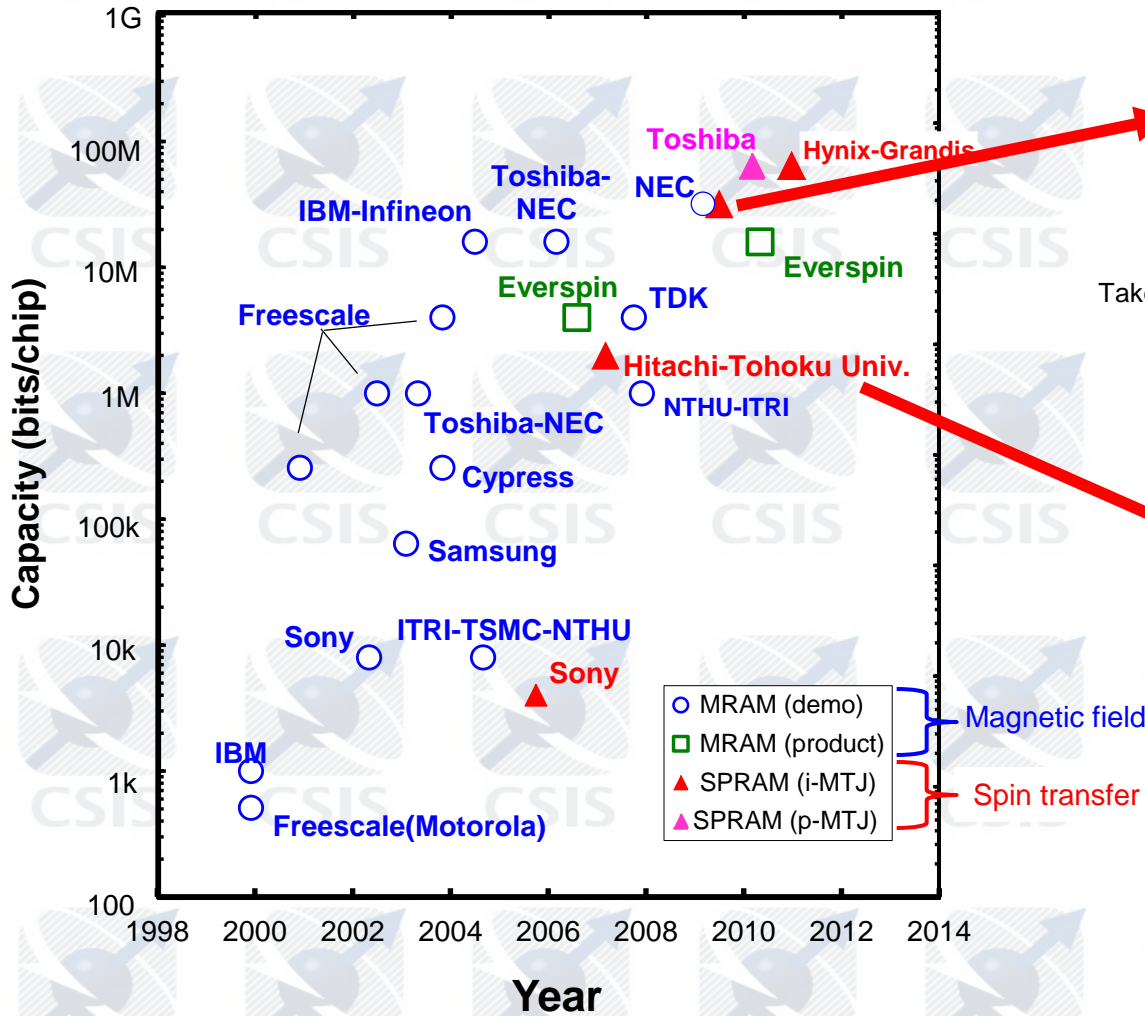
Matsunaga *et al.*, Appl. Phys. Express, 1 (2008) 091301; *ibid.*, 2 (2009) 023004.

Sekikawa *et al.*, IEDM 2008, Suzuki *et al.*, VLSI Technology 2009

Ohno *et al.*, IEDM 2010

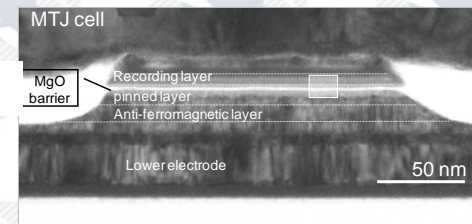
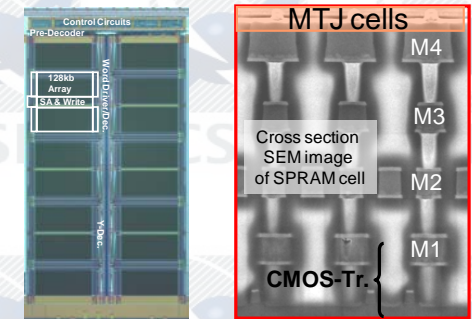
Matsunaga *et al.* VLSI Circuit 2011

MRAM development



32Mb SPRAM
VLSI Circuit 2009

Takemura et al., IEEE J. Solid-State Circuits 45 (2010) 869.

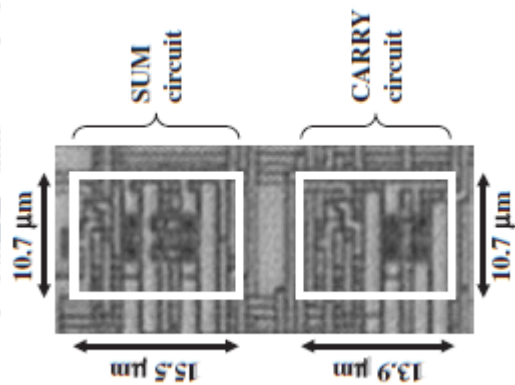


2Mb SPRAM
ISSCC 2007

Kawahara et al., IEEE J. Solid-State Circuits 43 (2008) 109.

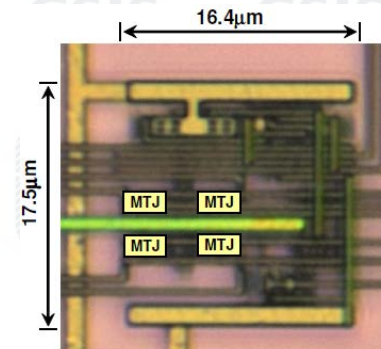
Ikeda et al., IEEE Trans. Electron Devices, 54 (2007) 991.

Nonvolatile circuits for logic-in-memory



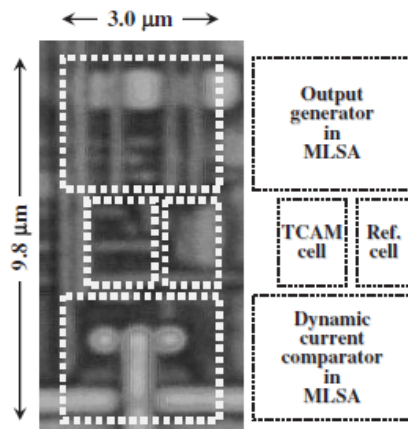
MTJ-Based
Nonvolatile Full
Adder

Matsunaga, ...Hanyu *et al.*,
Appl. Phys. Express 1 (2008) 091301.



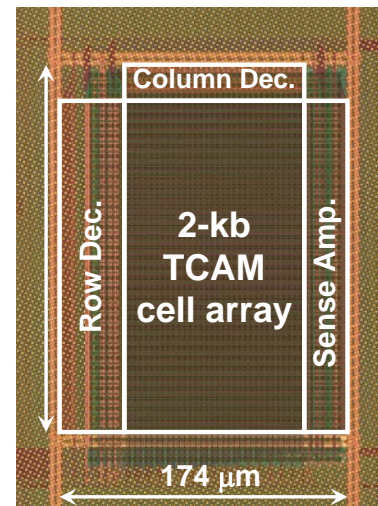
MTJ-Based Nonvolatile
Lookup-Table Circuit Chip

Suzuki, ...Hanyu, *et al.*, VLSI
Circuit Symposium 2009.



MTJ-Based
Nonvolatile
Ternary Content-
Addressable
Memory (TCAM)
cell

Matsunaga, ... Hanyu *et al.*, Appl. Phys.
Express 2 (2009) 023004.



2kb-nonvolatile
TCAM chip

Matsunaga, ...Hanyu, *et al.*,
VLSI Circuit Symposium 2011.

Technology issues toward realization of nonvolatile VLISs

To realize nonvolatile VLISs (MRAM and logic-in-memory) using the leading edge technology node, there are still issues to be addressed.

ISSUES

- High output (TMR ratio > 100%)
- Low switching current ($I_C < F \mu A$)
- Thermal stability for nonvolatility ($E/k_B T > 40$)
- Annealing stability
in back-end-of-line process ($T_a > 350^\circ C$)

+ Scalability

- MTJs have to satisfy these requirements with scalability at the same time.
- In order to satisfy these requirements, we focus on the MTJs with perpendicular anisotropy electrodes.

Progress of MTJs

CoFeB

MgO

CoFeB



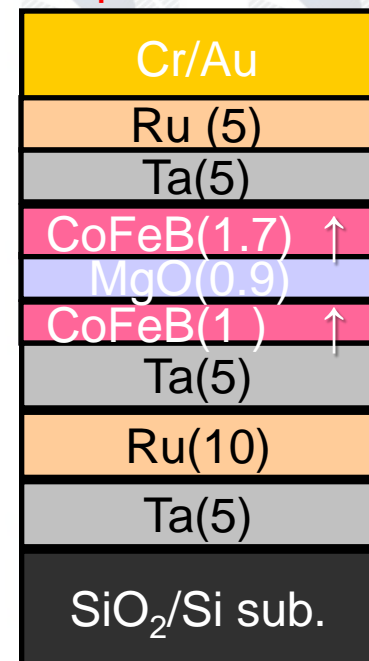
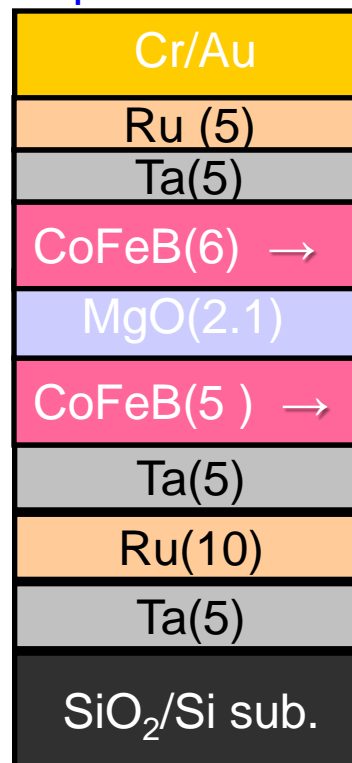
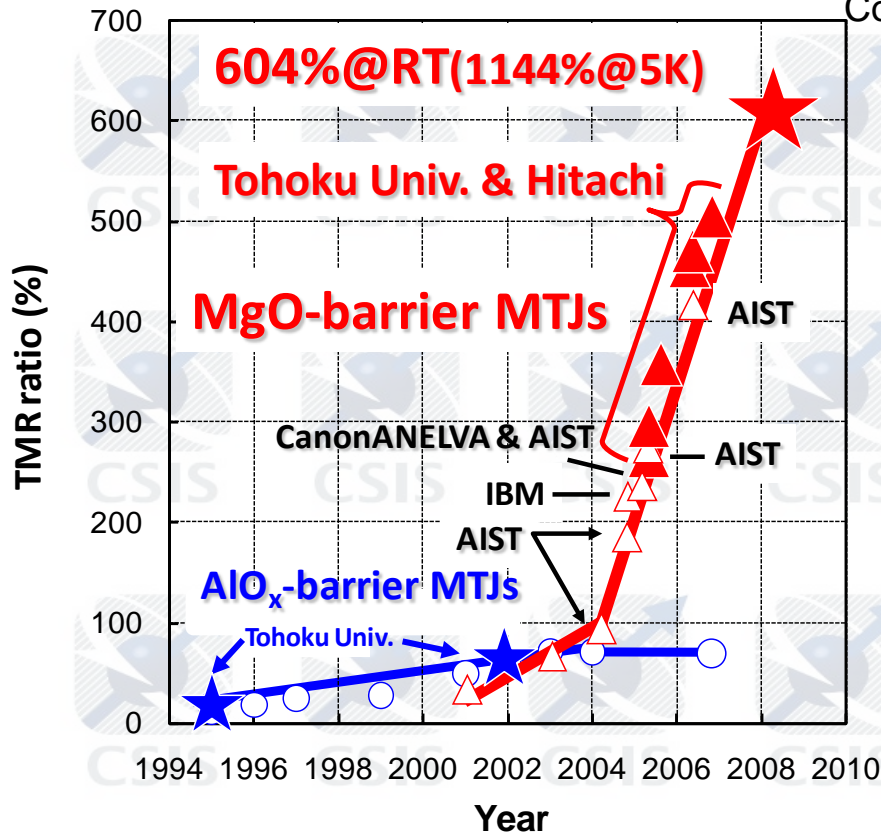
bcc (001)

rock salt (001)

bcc(001)

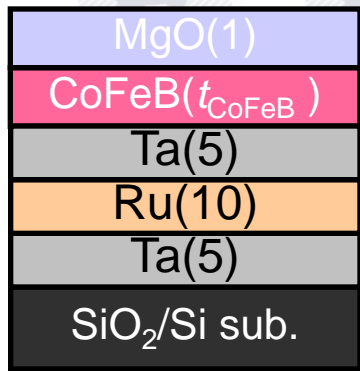
In-plane anisotropy
pseudo-SV

Perpendicular anisotropy
pseudo-SV

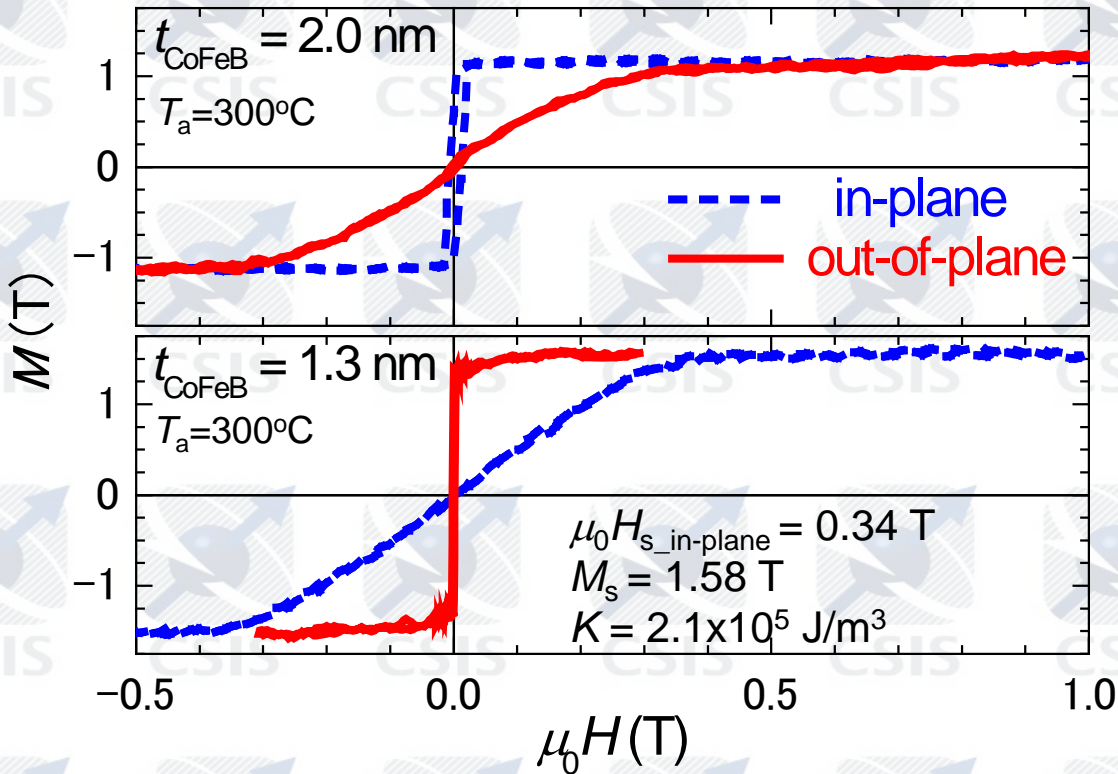


S. Ikeda et. al., Appl. Phys. Lett. **93**, 082508 (2008).
Nat. Mat., **9**, 721 (2010)

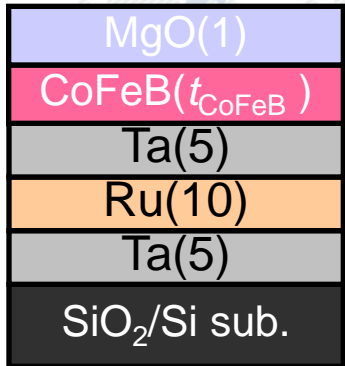
M-H curves of CoFeB/MgO stack samples with different t_{CoFeB}



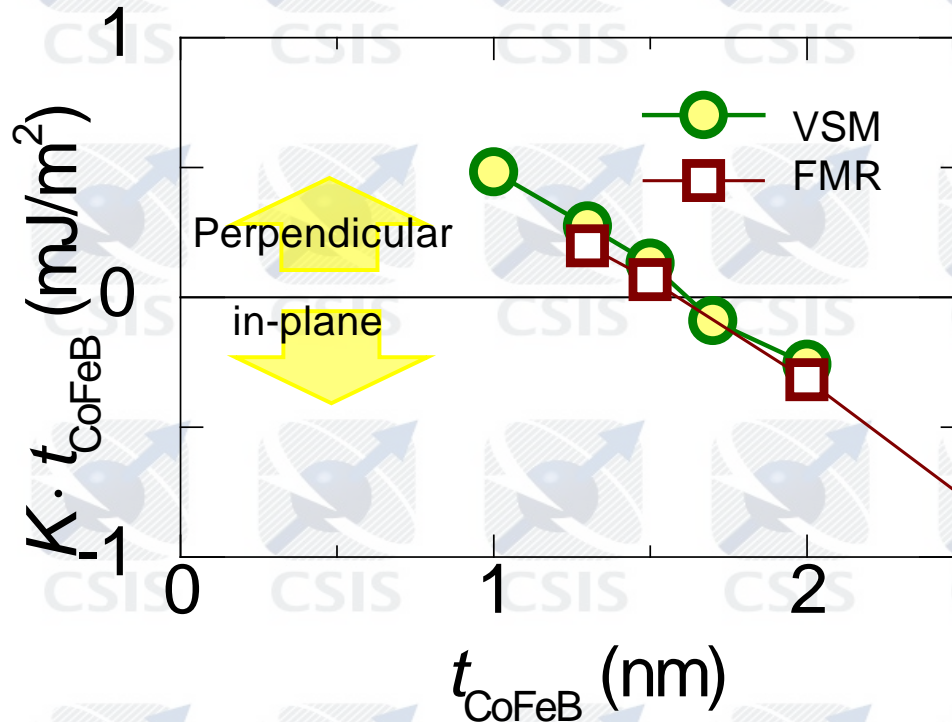
$T_a = 300^\circ\text{C}$,
4 kOe, 1h



t_{CoFeB} dependence of Kt_{CoFeB} in CoFeB/MgO stack



$T_a = 300^\circ\text{C}$

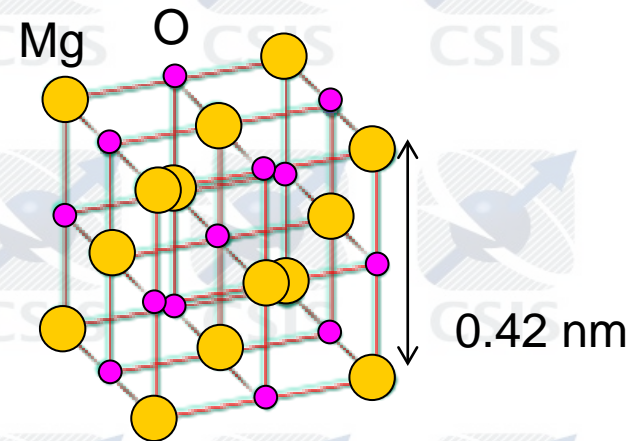
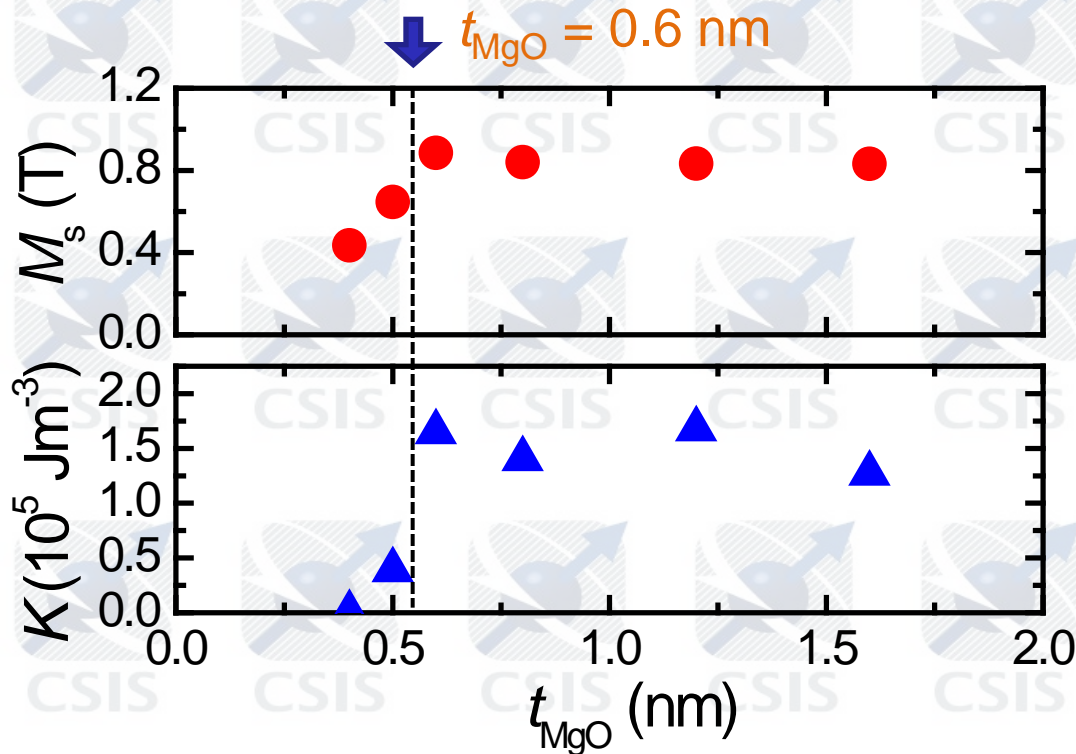


$$Kt_{\text{CoFeB}} = (K_b - M_S^2/2\mu_0) t_{\text{CoFeB}} + K_i$$

- From the y-intercept, $K_i = 1.3 \text{ mJ/m}^2$.
- The CoFeB/MgO interfacial anisotropy K_i is dominant in the perpendicular anisotropy because K_b is negligible.

t_{MgO} dependence of M_s and K

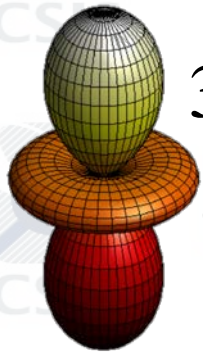
Saturation magnetization M_s and effective magnetic anisotropy energy density K are evaluated from the out-of-plane $M-H$ curves.



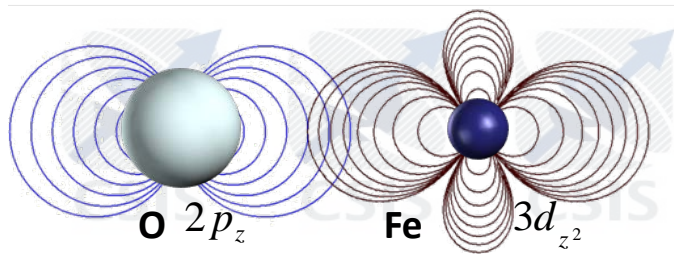
1 monolayer of MgO is $\sim 0.21 \text{ nm}$

More than 3 monolayers of MgO is required to stabilize the perpendicular anisotropy induced by CoFeB-MgO interface.

Possible factor of the perpendicular anisotropy in CoFeB/ MgO stack



$3d_{z^2}$: in-plane anisotropy
($m=0$)



anti-bonding

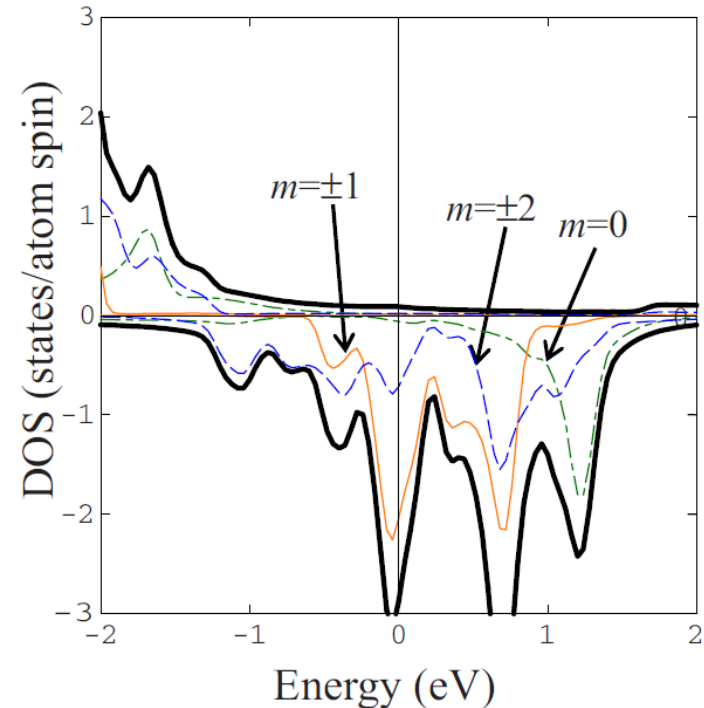
Fe $3d_{z^2}$ ($m=0$)

σ -coupling

O $2p_z$

bonding

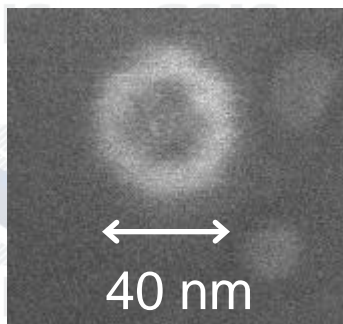
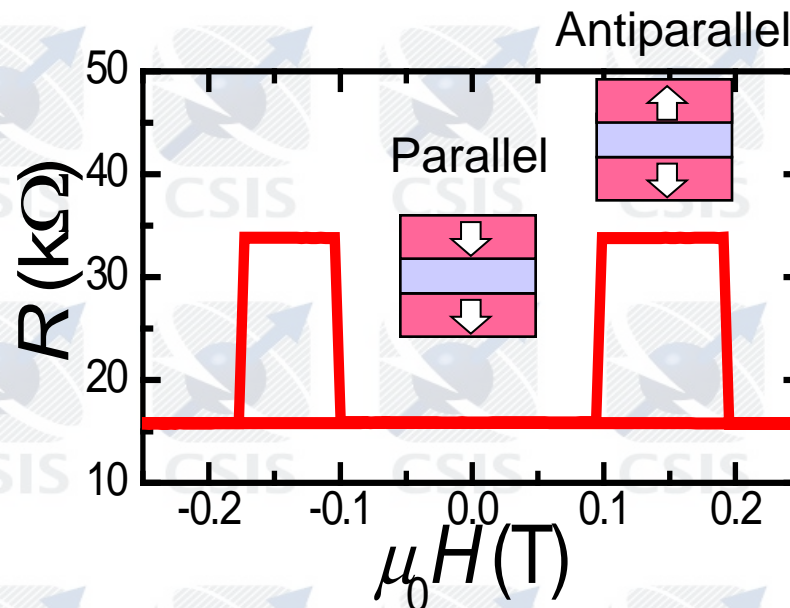
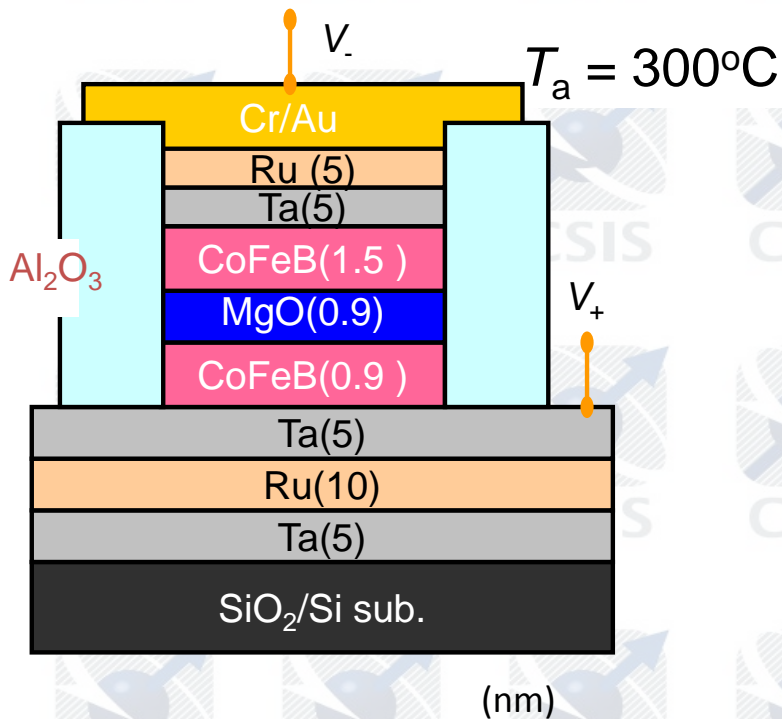
(a) Fe/MgO



K. Nakamura *et al.*, Phys. Rev. B, 81 (2010) 220409.
R. Shimabukuro *et al.*, Physica E 42 (2010) 1014.

- $3d_{z^2}$ band of Fe is pushed up above the Fermi energy.
- The contribution of $3d_{z^2}$ orbital of Fe becomes small, resulting in appearance of perpendicular anisotropy.

TMR properties in CoFeB-MgO p-MTJs



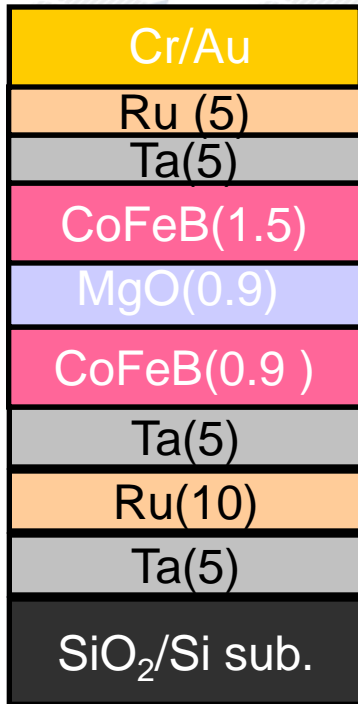
Clear hysteresis -> top and bottom CoFeB electrodes have perpendicular anisotropy.

Junction size dependence of I_{CO}

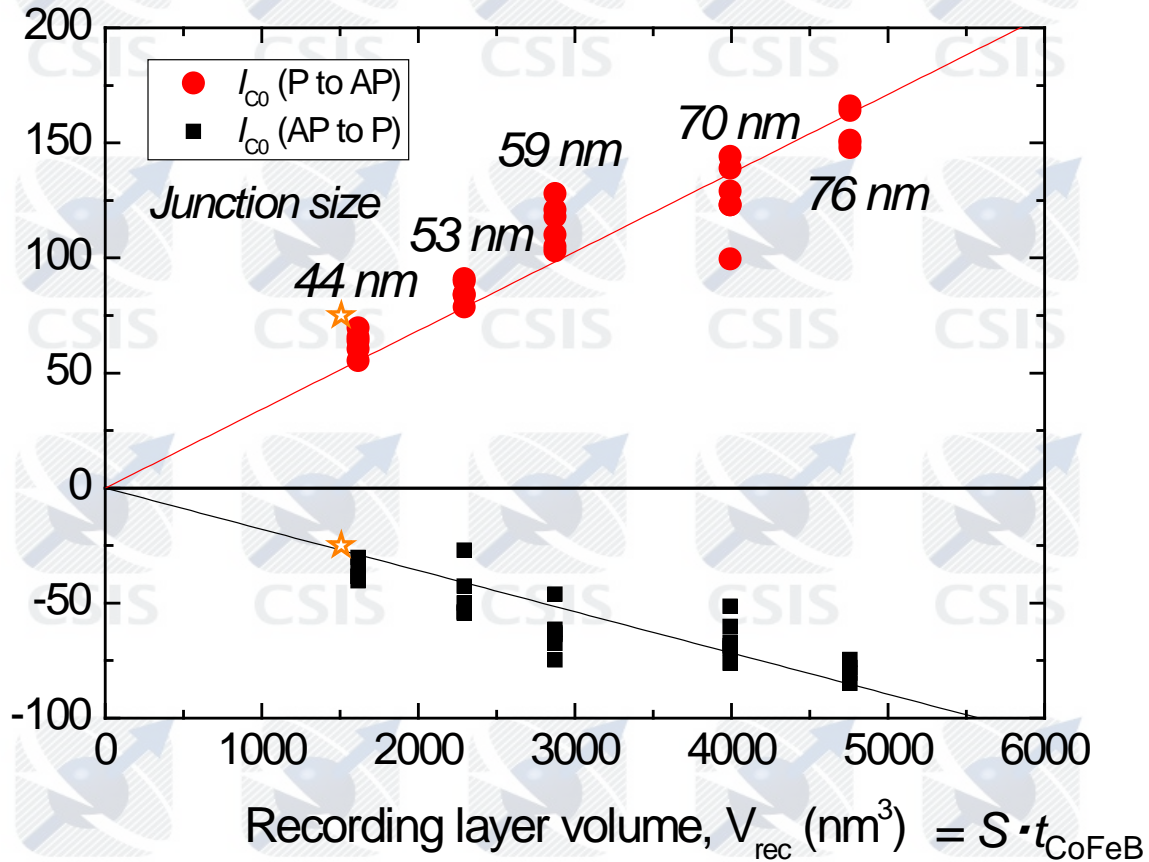
$F = 40 \sim 76 \text{ nm}\phi$

$T_a = 300^\circ\text{C}$

w/o H_{ex}

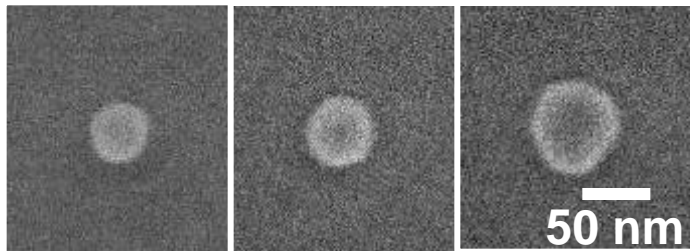


Critical current, I_{CO} (μA)

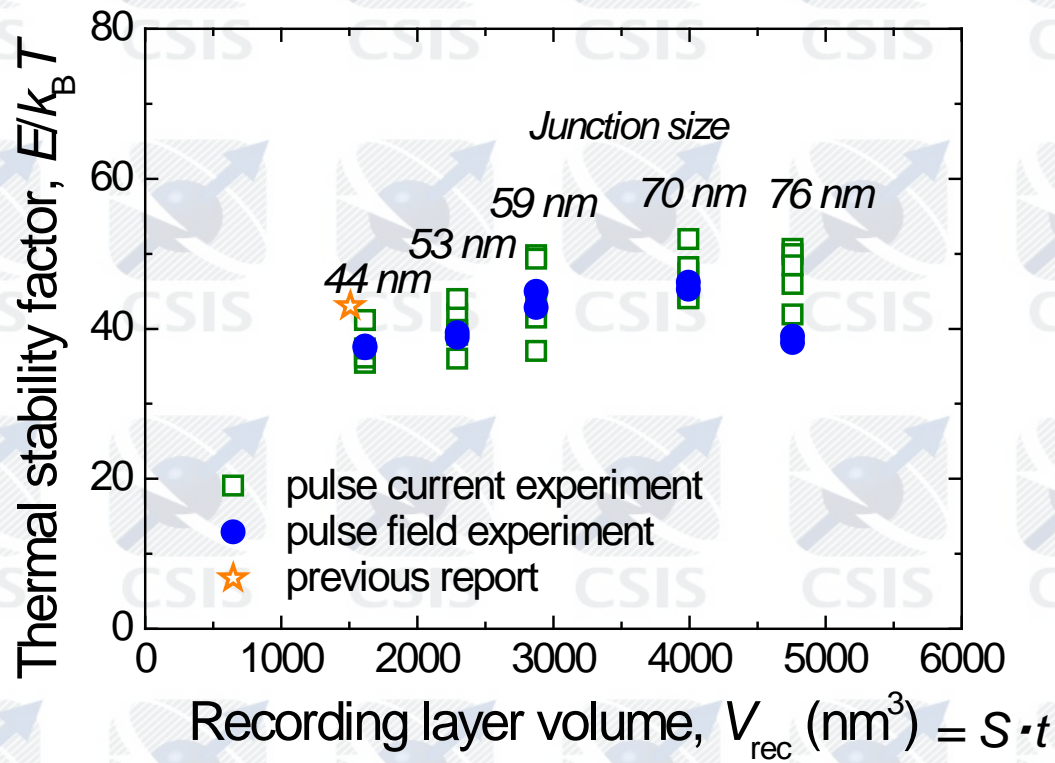


I_{CO} linearly decreases with junction area S (volume V_{rec}).

We confirmed scalability of switching current for spin transfer torque.



Junction size dependence of $E/k_B T$



$E/k_B T$ maintained almost constant values even though the junction diameter was varied from 40 nm to 80.

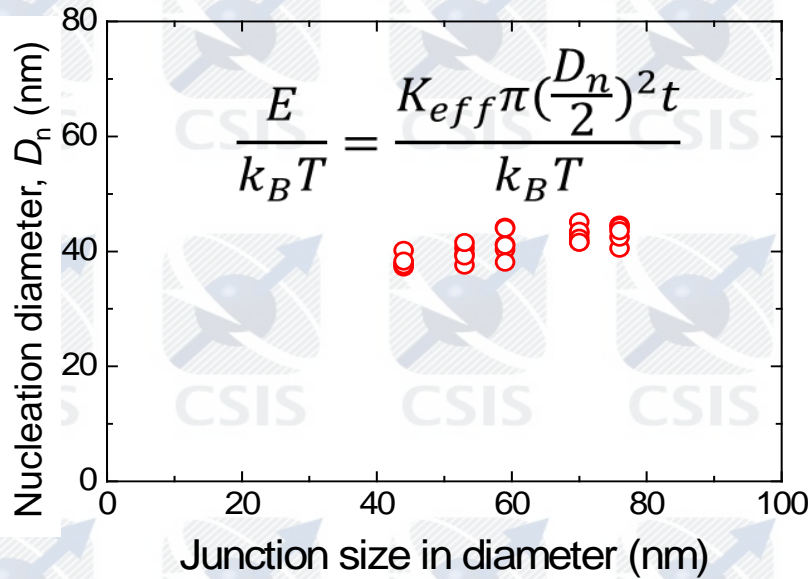
I_{C0} reduces in proportion to the volume of the recording layer but the $E/k_B T$ values are not affected much by the volume down to 40 nm in diameter.

Origin of the junction size dependence of I_{C0} and $E/k_B T$

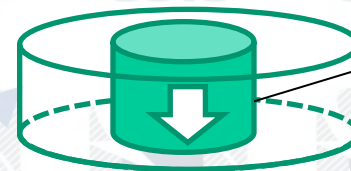
No clear reduction in $E/k_B T$ with different junction size



Nucleation type magnetization reversal



Junction area (diameter): $S(D)$



Nucleation embryo

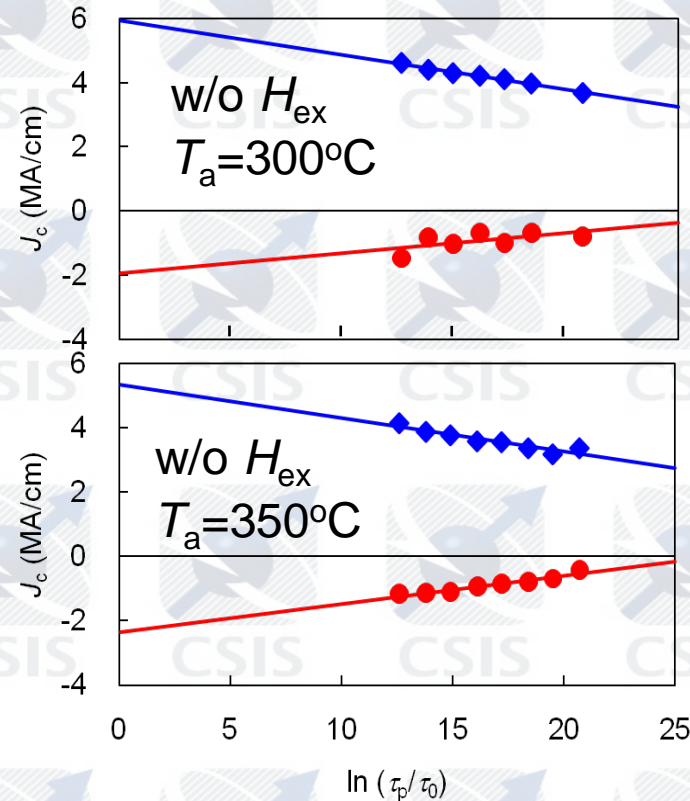
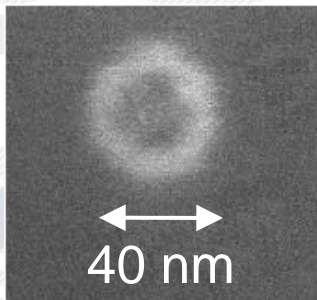
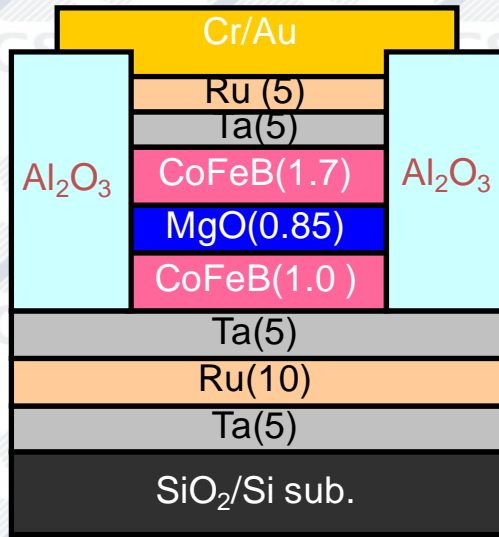
Nucleation diameter: D_n

D_n showed almost constant values of 40 nm in diameter, which is almost independent of junction size.

$$I_{C0} = J_{C0} S = J_{C0} (\pi(D^2 - D_n^2)/4) + \pi(D_n/2)^2 \propto S$$

$$E/k_B T = K_{eff} \pi(D_n/2)^2 / k_B T \propto D_n^2$$

J_{c0} and $E/k_B T$ of MTJs with 40 nm diameter



$T_a(^{\circ}\text{C})$	TMR ratio (%)	RA ($\Omega\mu\text{m}^2$)	J_{c0} (MA/cm^2)	$E/k_B T$
300	124	18	3.9	43.1
350	113	16	3.8	39.1

- J_{c0} and $E/k_B T$ are maintained after annealing at 350°C.
- This MTJ system has a back end of the line (BEOL) compatibility.

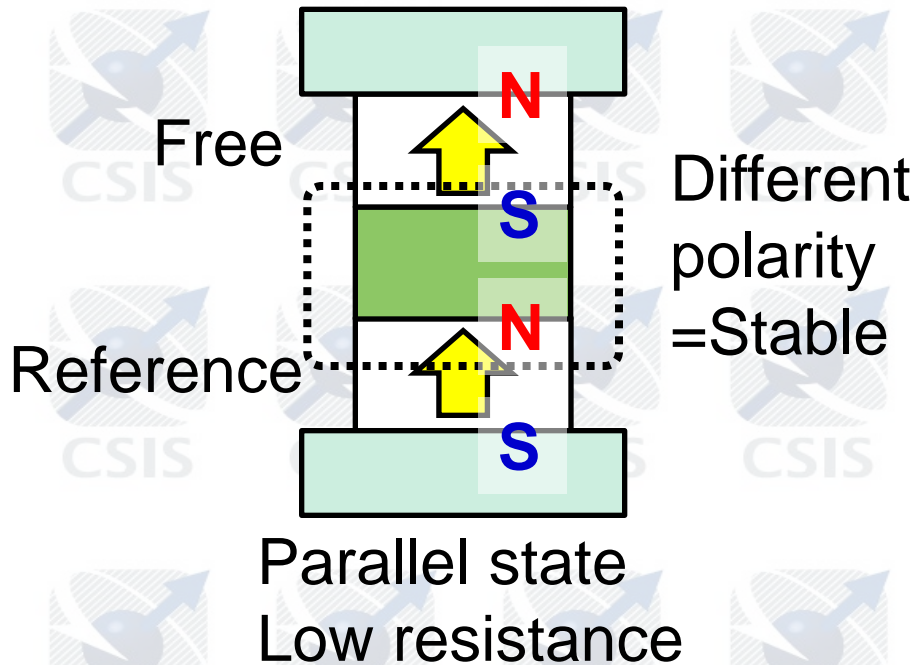
Comparison of MTJs

Type	Stack structure (nm)	Size (nm)	MR (%)	RA ($\Omega\mu\text{m}^2$)	J_{Co} (MA/cm^2)	I_{Co} (μA)	$\Delta=E/k_{\text{B}}T$	I_{Co}/Δ	T_{a} ($^{\circ}\text{C}$)	Ref.
i-MTJ	CoFeB(2)/Ru(0.65)/CoFeB(1.8) SyF	100x200	>130	~10	2	~400	65	~6.2	300-350	J. Hayakawa et al., IEEE T-Magn., 44, 1962 (2008)
p-MTJ	L10-FePt(10)/Fe(t)/Mg(0.4)/MgO(1.5)/L10-FePt(t)	Blanket	120 (CIPT)	11.8k	-	-	-	-	500	M. Yoshizawa et al., IEEE T-Magn., 44, 2573 (2008)
p-MTJ	L10-FePt/CoFeB/MgO(1.5)/CoFeB/Co based superlattice	Blanket	202 (CIPT)	-	-	-	-	-	-	H. Yoda et al., Magnetics Jpn. 5, 184 (2010) [in Japanese].
p-MTJ	[Co/Pt]CoFeB/CoFe/MgO/CoFe/CoFeB/TbFeCo	Blanket	85-97 (CIPT)	4.4-10	-	-	-	-	225	K. Yakushiji et al., APEX 3, 053033 (2010)
p-MTJ	[CoFe/Pd]/CoFeB/MgO/CoFeB/[CoFe/Pd]	800x800 N	100 (113)	18.7k (20.2k)	-	-	-	-	350 (325)	K. Mizunuma et al., MMM&INTERMAG2010
p-MTJ	CoFeB (1)/ TbCoFe (3)	130 ϕ	~15	-	4.7	650	107	6.08	-	M. Nakayama et al., APL 103, 07A710 (2008)
p-MTJ	L1 ₀ -alloy	50-55 ϕ	-	-	-	49	56	0.88	-	T. Kishi et al., IEDM 2008
p-MTJ	Fe based L1 ₀ (2)/CoFeB (0.5)	-	-	-	-	9	-	-	-	H.Yoda et al., Magnetics Jpn. 5, 184 (2010) [in Japanese].
p-MTJ	CoFeB/MgO/CoFeB	40 ϕ	113 (124)	16 (18)	3.8 (3.9)	48 (49)	39 (43)	1.23 (1.14)	350 (300)	S. Ikeda et al., Nat. Mat. 9 (2010) 721. K. Miura et al., MMM2010,HC-02

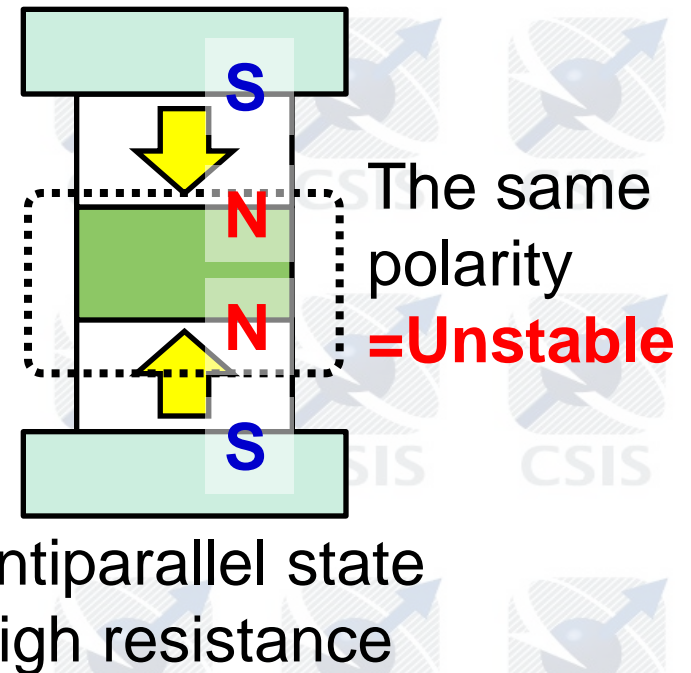
These p-MTJ technologies will be a promising building block for nonvolatile VLSIs using spin-transfer torque switching.

Issue for p-MTJs

Bit Information “0”



Bit Information “1”

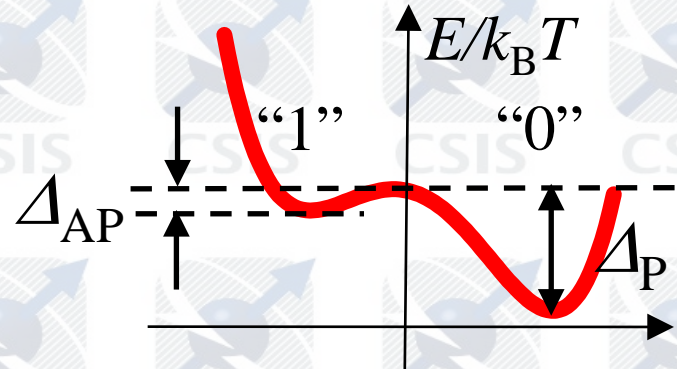
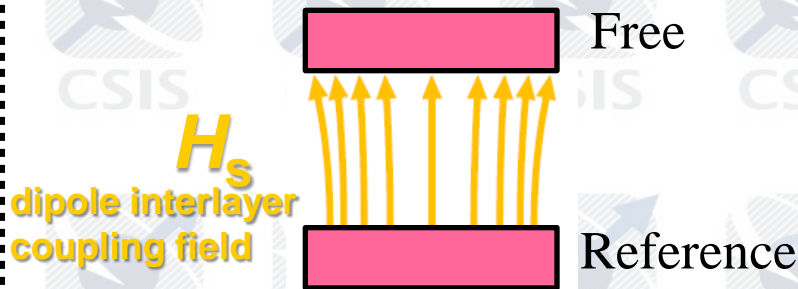


The thermal stability $\Delta_p = E/k_B T$ of anti-parallel state in p-MTJs becomes low by comparison with parallel state.

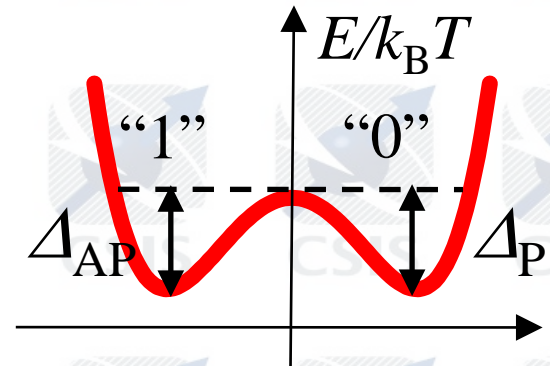
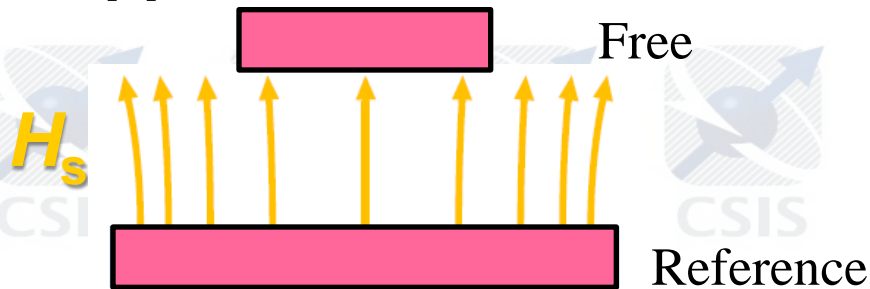
Enhancement of thermal stability

$$\Delta_{P, AP} = \Delta [1 \pm H_s/H_{c0}]^2$$

Conventional structure



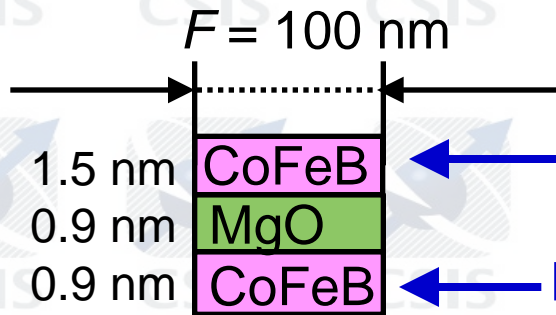
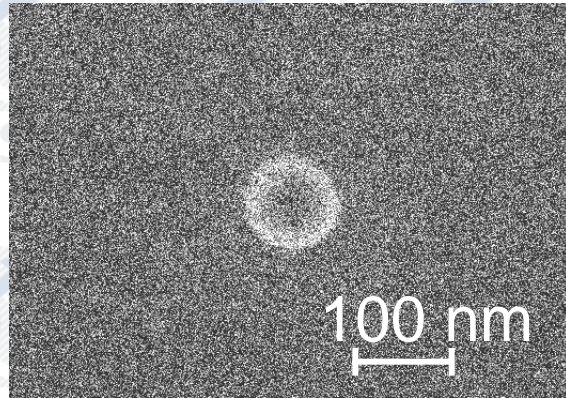
Stepped structure



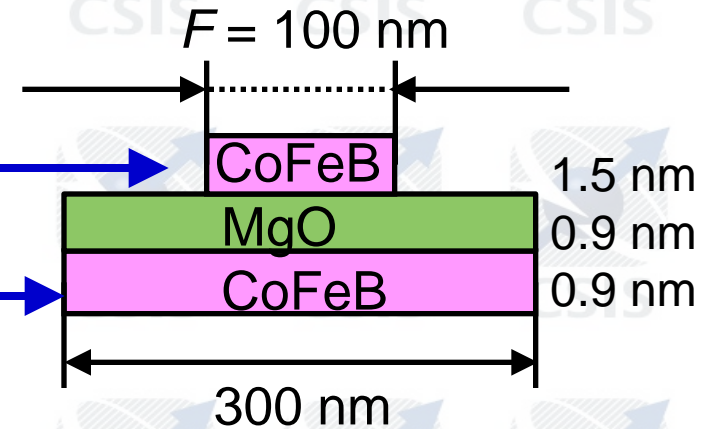
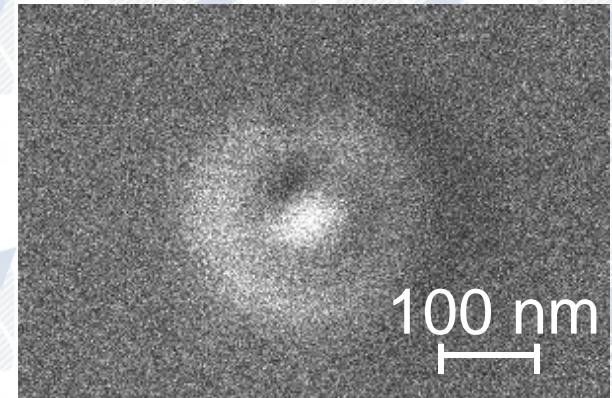
H_s decreases by employing step structure with large reference layer.
 Δ_{AP} increases with decreasing diameter of reference layer.

Two types of p-MTJs

Conventional structure

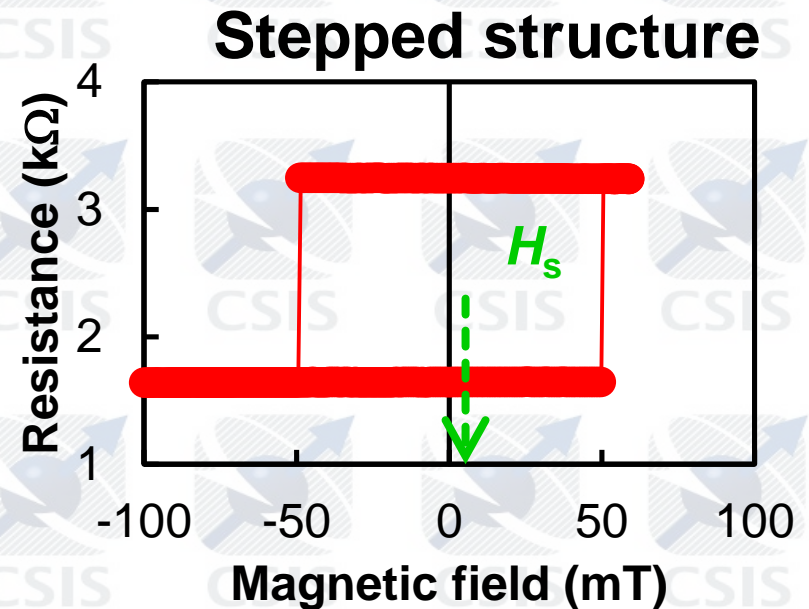
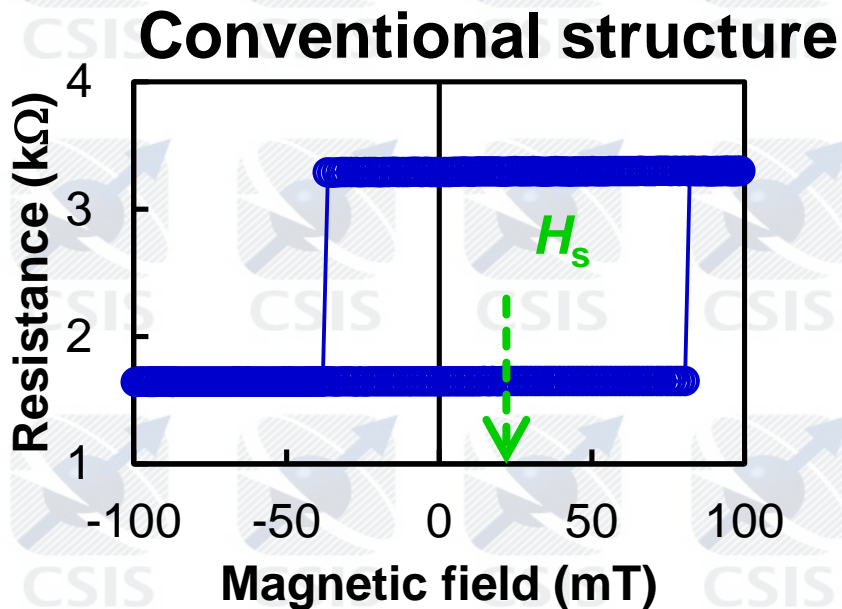


Stepped structure



F : Feature size

H_s in two types of p-MTJs



	Conventional structure	Stepped structure
TMR ratio (%)	100	97
RA ($\Omega\mu\text{m}^2$)	13	13
H_s (mT)	22	5

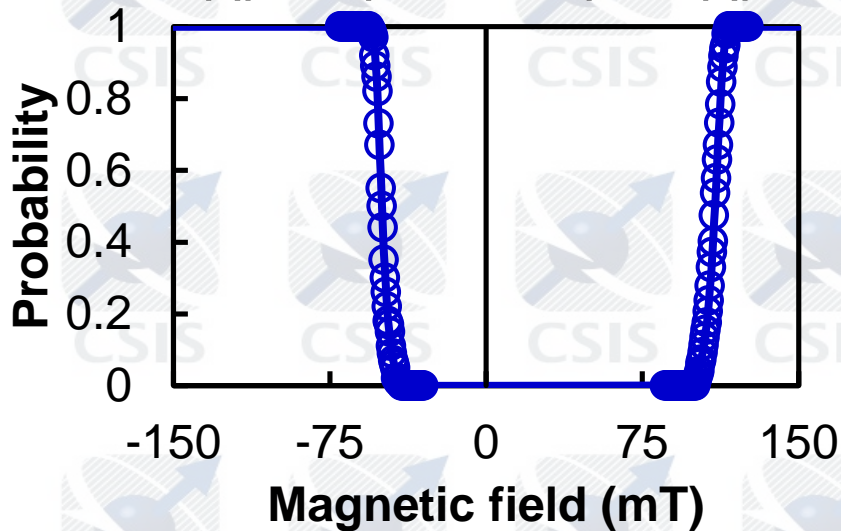
H_s can be reduced by using stepped structure.

Δ_P and Δ_{AP} in two types of p-MTJs

$$\text{Probability} = 1 - \exp \left\{ 1 - \frac{\tau_p}{\tau_0} \exp \left[\Delta \left(1 - \frac{H - H_s}{H_{c0}} \right)^2 \right] \right\} \quad \Delta_{P,AP} = \Delta \left(1 \pm \frac{H_s}{H_{c0}} \right)^2$$

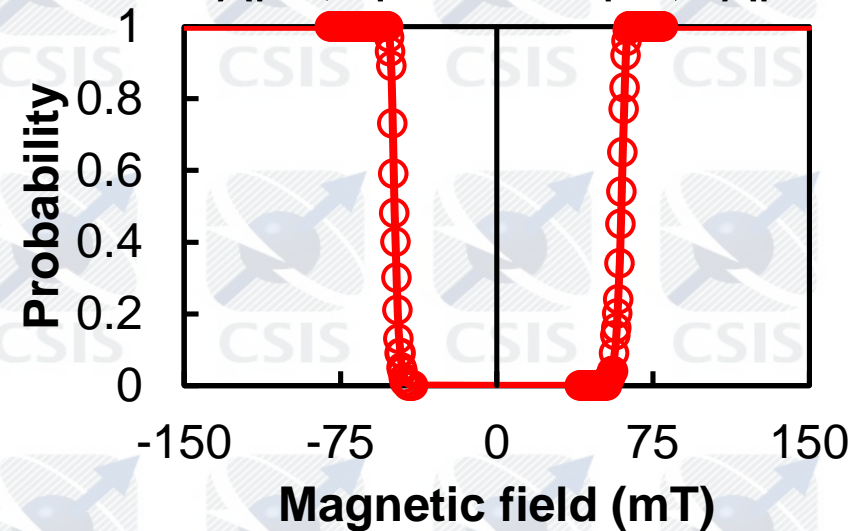
Conventional structure

“AP”->”P” “P”->”AP”



Stepped structure

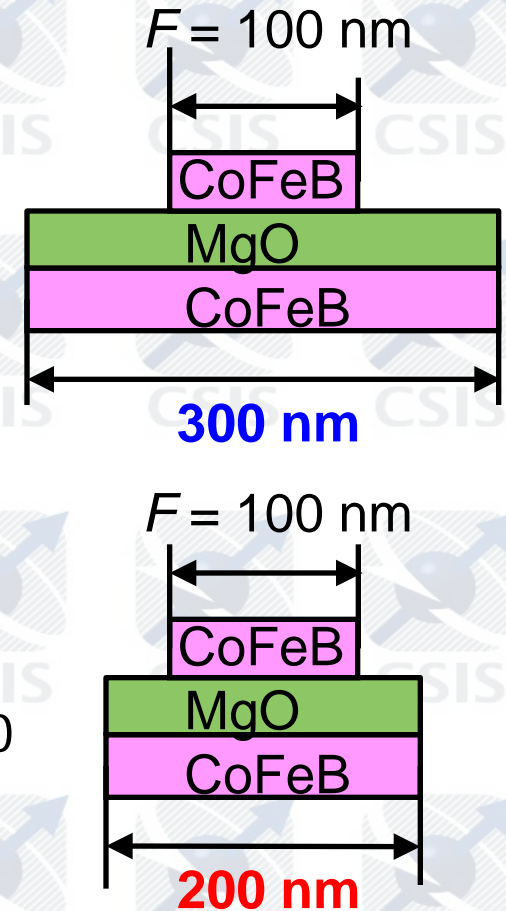
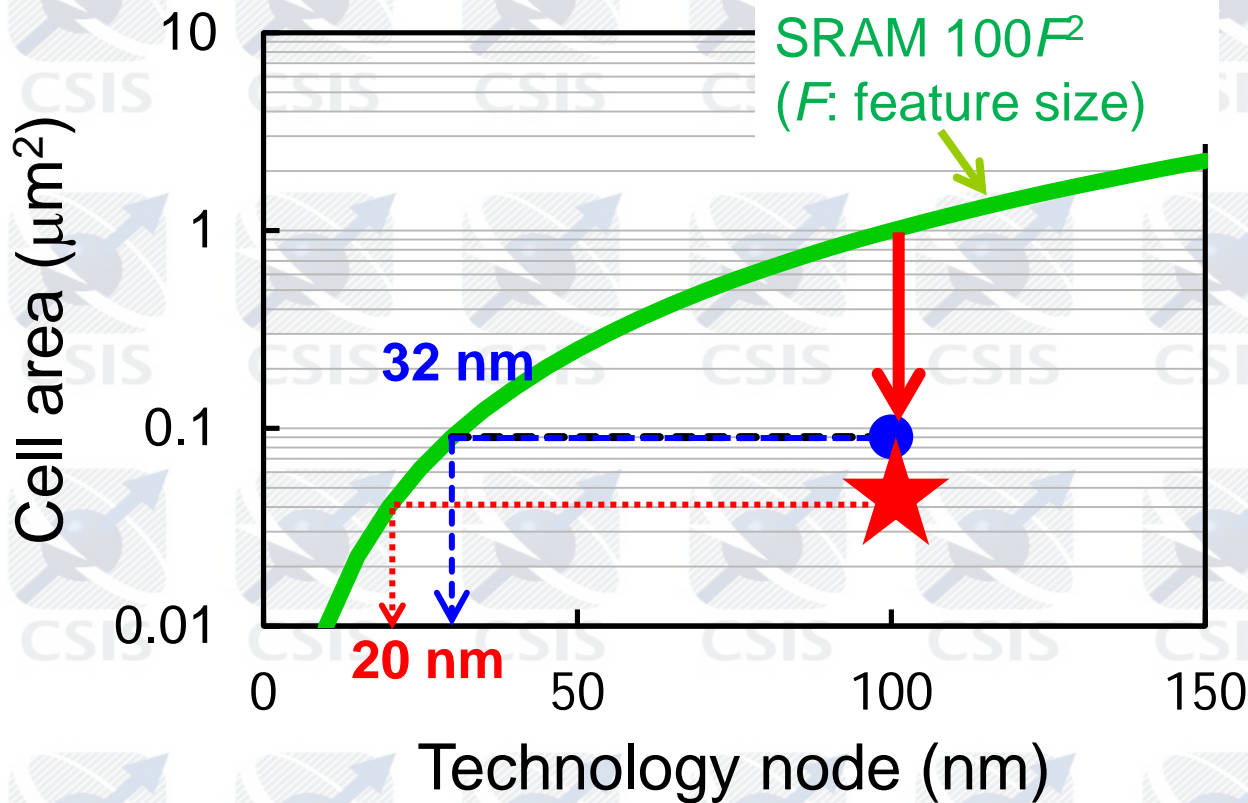
“AP”->”P” “P”->”AP”



	Conventional structure	Stepped structure
Δ_P	71.2	72.9
Δ_{AP}	46.5	70.1

Δ_{AP} in stepped structure increases.

Cell area of stepped structure



Cell area of $0.09 \mu\text{m}^2$ ($300\text{nm}\phi$) in the stepped structure corresponds to SRAM cell area at 32 nm technology node.

Cell area can be down to $0.04 \mu\text{m}^2$ ($200\text{nm}\phi$) without degrading the retention time over 10 years, which corresponds to SRAM cell area at 20 nm technology node.

Summary

- We have demonstrated that the critical current I_{c0} in CoFeB/MgO perpendicular anisotropy MTJs (p-MTJs) can be scaled down with decreasing recording layer volume.
- The thermal stability factor $E/k_B T$ can be maintained at about 40 even though the recording volume was reduced to 40 nm. The magnetization reversal in CoFeB/MgO p-MTJs is dominated by nucleation type magnetization reversal (nucleation diameter ~40 nm).
- CoFeB/MgO p-MTJs show the high TMR ratio of more than 100%, high thermal stability at dimension as low as 40 nm diameter and a low switching current of 49 μ A at the same time .
- CoFeB/MgO p-MTJ with step structure shows the enhancement of thermal stability in antiparallel state, which achieves thermal stability for data retention time over 10 years.